Triggering Redox Activity in a Thiophene Compound: Radical Stabilization and Coordination Chemistry

Triggering Redox Activity in a Thiophene Compound: Radical Stabilization and Coordination Chemistry

Massimiliano Curcio,[a] James R. Pankhurst,[a] Stephen Sproules,[b] Dimitri Mignard,[a] and Jason B. Love*[a]

Abstract: The synthesis, metalation, and redox properties of an acyclic bis(iminothienyl)methene **L**$^-$ are presented. This π-conjugated anion displays pronounced redox activity, undergoing facile one-electron oxidation to the acyclic, metal-free, neutral radical **L**$^\bullet$ on reaction with $FeBr_2$. In contrast, reaction of **L**$^-$ with CuI forms the unique, neutral Cu_2I_2(**L**$^\bullet$) complex of a ligand-centered radical, whereas reaction with the stronger oxidant $AgBF_4$ forms the metal-free radical dication **L**$^{\bullet 2+}$.

Since the first reports on dithiolate metal complexes,[1] interest in redox-active ligands has burgeoned due to their relevance to enzymatic processes[2] and access to unusual chemical properties by coupling the redox activity of the ligand to the coordination chemistry of a metal.[3] In these cases, the ligand is no longer a classical "spectator",[4] and a large number of ligands have been shown to exhibit redox activity and stabilize the radical species through an inductive effect or by delocalization in a conjugated π-system.

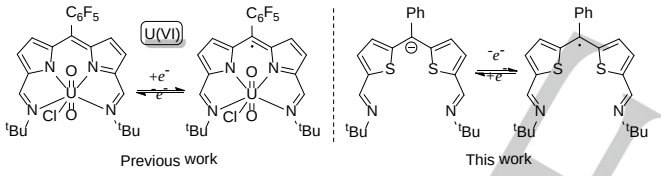

Figure 1. Left: A uranium complex of a redox-active bis(iminopyrrolyl)methene ligand. Right: A redox-active bis(iminothienyl)methene.

Accordingly, we have shown that an N-donor-expanded dipyrrin ligand[5] is redox active and able to mediate sequential electron transfer to a uranyl(VI) center (Figure 1). The initial reduction occurs at the ligand, forming a U(VI) ligand-centered radical prior to reduction of the uranium center, ultimately to U(IV).[6] Ligand-centered oxidation was also seen in Ni complexes of a similar bis(phenolate)dipyrrin ligand, with the one-electron oxidation product characterized as a ligand-centered radical.[7]

In contrast to the nitrogen-containing heterocycles found in dipyrrins, porphyrinoids and sub-porphyrins,[8] studies on the redox activity of sulfur-containing heterocycles such as thiophene are more limited,[9] despite their use in tuning the electronic properties of molecular compounds[10] and polymeric materials.[11] Expanded porphyrinoids featuring five thiophene units undergo single-electron oxidations, from the aromatic mono-anion to an isolable, air-stable neutral radical, and further to an anti-aromatic mono-cation.[12] In contrast, radical cations of simple thiophenes or their analogues are stable only at low temperatures or their identity inferred from quenching reactions.[13, 14] We were keen to see if we could exploit redox activity and the 'softer' donor properties of the sulfur atoms in methylene-bridged thiophenes to access new transition-metal chemistry and reactivity. As such, we show here that the bis(iminothienyl)methene **L**$^-$ reacts with metal salts to generate the neutral radical **L**$^\bullet$, the dicationic radical **L**$^{\bullet 2+}$ or the dinuclear copper(I) complex Cu_2I_2(**L**$^\bullet$) of a ligand-based iminothienyl radical.

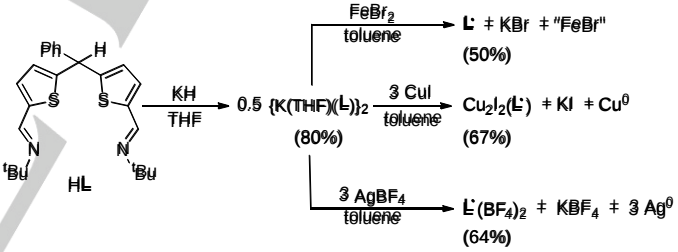

Scheme 1. Synthetic pathway to the monoanionic iminodithiophene K**L** and its redox reactions with metal salts (isolated yields in parentheses).

Studies on the *meso*-C lithiation of dithiophenemethane compounds have found thermodynamic *versus* kinetic selectivity issues along with the formation of *meso*-C coupled products.[15] However, we find that deprotonation of H**L** with KH in THF selectively forms the highly moisture-sensitive potassium salt K**L** as green crystals in high yield (Scheme 1).

The X-ray structure reveals a dimeric structural motif in the solid state (Figure 2). The two imino-thiophene ligands adopt a dinuclear mesocate arrangement at the K centers. The K-S distances appear long (> 3.3 Å), but as no other K-S(thiophene) compounds exist no comparisons can be made. The deprotonated ligand shows extended π-conjugation, evident from the planar arrangement of the ligand components linked by the sp^2 hybridized *meso*-carbon C10; the dihedral angle between iminothienyl planes is 5.9° and the C9-C10 and C10-C17 distances are shortened by 0.1 Å in comparison to the sp^3-hybridized H**L** (SI). This unusual dinuclear coordination motif is likely related to the large separation of the imine nitrogen donor

[a] M. Curcio, J. R. Pankhurst, Dr. D. Mignard, Prof. J. B. Love
EaStCHEM School of Chemistry and School of Engineering
University of Edinburgh, The King's Buildings
Edinburgh, EH9 3FJ (UK)
E-mail: Jason.Love@ed.ac.uk
[b] Dr. S. Sproules
WestCHEM School of Chemistry
University of Glasgow
Glasgow G12 8QQ (UK)

Supporting information for this article is given via a link at the end of the document.

atoms (N1···N2 = 7.357(1) Å) as a consequence of incorporating the thiophene heterocycles. This is evidenced by comparison with the X-ray crystal structure of the analogous potassium iminodipyrrin K(L^{N4}) in which the K cation is coordinated to all four N atoms of the ligand, with an imino N1···N4 separation of 5.513(2) Å (Figure S18).

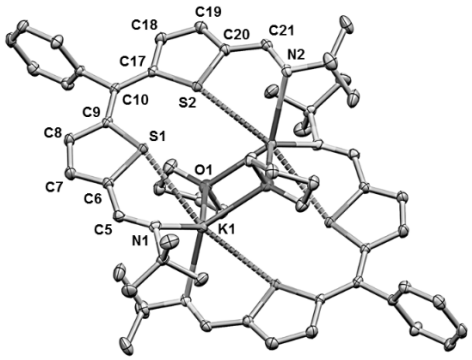

Figure 2. Solid-state structure of K**L**. For clarity, all hydrogen atoms and a molecule of benzene solvent are omitted (displacement ellipsoids are drawn at 50% probability). Selected bond lengths (Å) and angles (°): S1-K1 3.3461(6), N1-K1 2.821(1), N1-C5 1.290(1), S2-K1 3.3676(5), N2-K1 2.852(1), N2-C21 1.289(1), C9-C10-C17 127.3(1), S1-K-N1 58.96(2), S2-K-N2 59.18(2).

The availability of K**L** allowed reactions with transition metal salts to be explored (Scheme 1). The reaction between K**L** and $FeBr_2$ did not lead to the metathesis product FeBr(**L**) but instead results in the neutral, toluene-soluble, metal-free radical **L**•. This highlights the poor coordinating ability of the thiophene ligand compared to its dipyrrin analogue. The radical **L**• is isolated as dichroic yellow/green crystals from toluene and its solid-state structure determined (Figure 3, left), from which it is clear that the *meso*-carbon C10 is sp^2 hybridized with delocalized C9-C10 and C10-C17 bonds. Furthermore, the two iminothienyl planes are coplanar (torsion angle of 2.2°), suggestive of extended π-conjugation across the molecule. The radical nature of **L**• is supported by its fluid-solution EPR spectrum in CH_3CN, which shows a resonance at g = 2.0034, consistent with an organic radical (Figure 4). The weakly resolved hyperfine arises from coupling of the unpaired electron to six ^{1}H (I = $^1/_2$) and two ^{14}N (I = 1) nuclei, simulated with A^N = 3.02 × 10^{-4} cm^{-1} and three sets of protons, A^H = 1.43, 1.24, 0.71 × 10^{-4} cm^{-1}, and consistent with the calculated spin-density distribution (Figure 5). EPR spectra of samples diluted in CH_2Cl_2, toluene and THF suffer from perturbed molecular tumbling which leads to line broadening that generates featureless signals. While the existence of the radical cations of benzannulated thiophene heterocycles has been probed by trapping with O_2,[13] only one example of an isolable neutral thiophene radical has been reported to date by taking advantage of stabilization by delocalization throughout a macrocyclic framework;[12] therefore, to the best of our knowledge, compound **L**• is the first isolable acyclic, neutral thiophene radical.

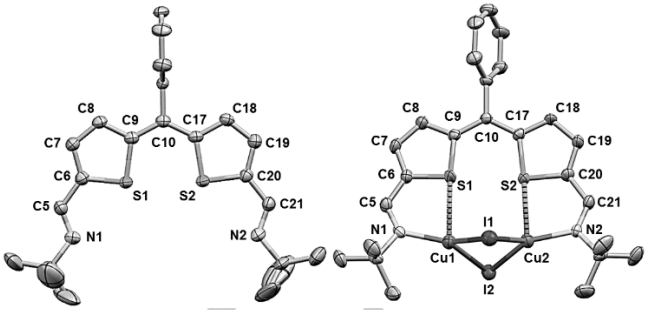

Figure 3. Solid-state structures of **L**• (left) and Cu_2I_2(**L**•) (right). For clarity, all hydrogen atoms are omitted (displacement ellipsoids are drawn at 50% probability). Selected bond lengths (Å) and angles (°): **L**• N1-C5 1.280(4), C5-C6 1.428(5), S1-C6 1.729(3), S1-C9 1.752(3), C6-C7 1.378(5), C7-C8 1.381(5), C8-C9 1.401(4), C9-C10 1.423(5), C9-C10-C17 126.4(3); Cu_2I_2(**L**•) S1-Cu1 2.679(2), N1-Cu1 1.982(1), Cu1-I1 2.587(7), Cu1-I2 2.625(9), S2-Cu2 2.689(2), N2-Cu2 1.969(4), Cu2-I1 2.564(6), Cu2-I2 2.587(9), N1-C5 1.283(3), N2-C21 1.290(6), C9-C10-C17 125.8(8), S1-Cu1-N1 79.1(2), S2-Cu2-N2 80.3(2), N1-Cu1-I1 128.7(2), N1-Cu1-I2 129.3(2), Cu1-I1-Cu2 72.72(4), Cu1-I2-Cu2 71.73(4), I1-Cu1-I2 101.29(5), I1-Cu2-I2 102.96(5).

The reaction between K**L** and CuI results in both a precipitate of KI and reduction of Cu(I) to Cu metal but, unlike the reaction with Fe, the metalated product Cu_2I_2(**L**•) is isolated from toluene as a red powder. The solid-state structure was determined by X-ray crystallography and confirms its dinuclear nature,[16] with each Cu center adopting a distorted trigonal pyramidal geometry with the thienyl-S atom axial and imino-N and bridging-I atoms equatorial (Figure 3, right). As with K**L** and **L**•, the *meso*-carbon C10 is sp^2 hybridized with the two iminothienyl fragments essentially coplanar (7.9°). While the Cu-S distance is within the range (2.336 – 3.014 Å) seen for the five other Cu-thiophene complexes,[17] Electron Localization Function (ELF) calculations suggest that no covalent bond interaction between S and Cu occurs as the lone-pair character on S is directed away from the Cu-S vector (Figure S28). The paramagnetism of Cu_2I_2(**L**•) could conceivably arise from either the presence of the ligand radical **L**• and two Cu(I) centers, or from an anionic ligand with delocalized Cu(I)/Cu(II) mixed-valence cations. While mixed-valence Cu complexes have been reported and are seen to adopt *pseudo*-tetrahedral geometries in the solid state,[18] the fluid-solution EPR spectrum of Cu_2I_2(**L**•) shows a resonance at g = 1.9958 that is consistent with a ligand-based radical. The lowering of the g-value compared to **L**• is ascribed to spin-orbit contributions from the copper atoms which reduce all g-values to slightly less than g_e, as described by the frozen-solution spectrum (Figure S8). The lack of hyperfine structure may stem from overlapping coupling to the many spin-active nuclei (^{1}H, ^{14}N, ^{63,65}Cu, ^{127}I) in the system. Interestingly, the EPR spectrum in CH_3CN is similar to that of the radical **L**•, showing that the complex is labile in strong donor solvents (Figure S9).

The reaction between K**L** and $AgBF_4$ salt provides the dication **L**•$(BF_4)_2$ as the sole paramagnetic red/orange product. In the solid-state structure, **L**•$(BF_4)_2$ displays a planar arrangement of atoms, with essentially coplanar thienyl moieties (4.3°) (Figure S17. Note, due to the poor data quality only connectivity can be inferred). Interestingly, one of the BF_4 anions is accommodated

within the N_2S_2 molecular cleft and interacts with the imine nitrogen atoms with approximate distances of 2.78 Å (N1···F1) and 2.88 Å (N2···F3). The EPR spectrum of **L**$^{\bullet}$$(BF_4)_2$ is simulated with g = 2.0037, which is identical to **L**$^{\bullet}$. However, the hyperfine splitting pattern is less congested and the spectral profile was modelled with coupling to the ^{14}N nucleus (A^N = 2.38 × 10^{-4} cm^{-1}) and three protons (A^H = 3.22, 1.10, 0.70 × 10^{-4} cm^{-1}) of *one* iminothienyl arm. The spin-density distribution calculated for **L**$^{\bullet 2+}$ (Figure 5) corroborates this spectrum, showing spin density on one thiophene-imine arm only due to the twist at the *meso*-carbon atom (dihedral angle 50.9°) in the optimized structure. This calculated structure is different to that seen in the X-ray crystal structure of **L**$^{\bullet 2+}$ which is planar, presumably due to the presence of the BF_4^- counter-ion which interacts with both imine nitrogen atoms.

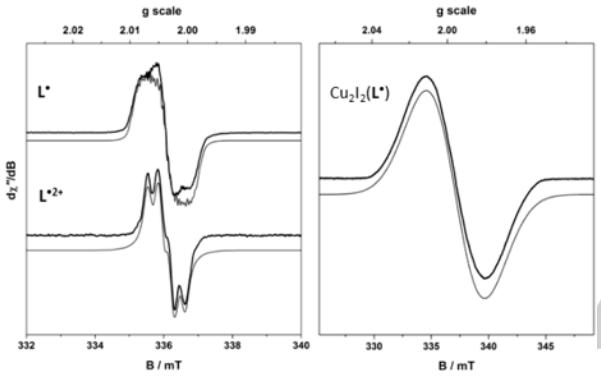

Figure 4. Fluid-solution X-band EPR spectra of radical ligands **L**$^{\bullet}$ and **L**$^{\bullet}(BF_4)_2$ in CH_3CN (left) and Cu_2I_2(**L**$^{\bullet}$) in CH_2Cl_2 (right) at 293 K. Experimental data are depicted by the black trace and simulations by the grey trace (simulation parameters are given in the text).

Upon deprotonation of H**L** to form K**L**, an intense band at 654 nm appears (Figure 5), and is similar, although red-shifted, to the HOMO-LUMO transition in related dipyrromethene compounds;[6] the band seen at 295 nm is indicative of re-protonation of K**L** and highlights its sensitivity to water. Oxidation of K**L** to the radical **L**$^{\bullet}$ results in a considerable hypsochromic shift of the low-energy absorption band, from 654 to 456 nm, which is explained by an increase in the SOMO(α)-LUMO(α) gap from TD-DFT calculations, from 4.41 keV in K**L** to 5.41 keV in **L**$^{\bullet}$. Incorporation of the dinuclear core in Cu_2I_2(**L**$^{\bullet}$) leads to the appearance of additional absorption bands, in particular a broad absorption at 826 nm (765 nm in the calculated spectrum) mainly involving the SOMO(β)-LUMO(β) transition. Although the UV-vis spectra are generally well-modeled by TD-DFT simulations, the transitions in Cu_2I_2(**L**$^{\bullet}$) involve the participation of a multitude of orbitals and cannot be straightforwardly assigned.

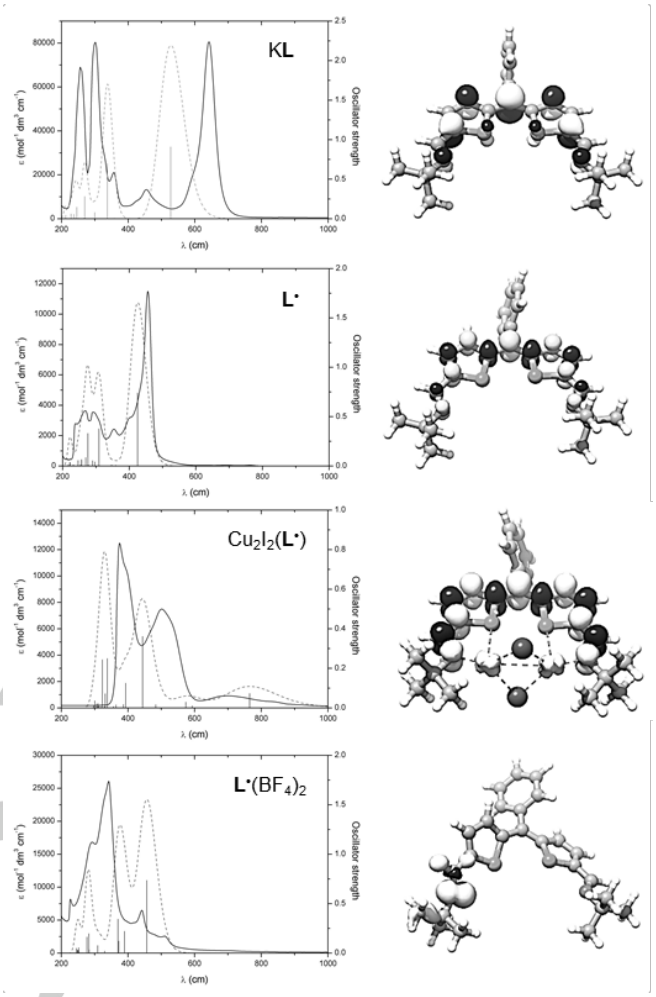

Figure 5. Left: experimental UV-vis spectra (black trace), TD-DFT calculated spectra (grey dashed trace) and oscillators (vertical lines). Right: DFT calculated HOMO for K**L** and spin-density plots for **L**$^{\bullet}$, Cu_2I_2(**L**$^{\bullet}$), and **L**$^{\bullet 2+}$.

While the cyclic voltammogram (CV) of H**L** displays a single irreversible reduction at E_p^c –1.46 V versus ferrocene (Figure S11), the CV of K**L** consists of two reversible events, with an oxidation at –0.12 V and a reduction at –1.33 V (Figure 6). These are complimentary to the reduction wave at –0.02 V in the CV for **L**$^{\bullet}$, together with another reduction at –1.38 V, assigned by linear-sweep voltammetry; in this case, the data profiles are skewed, indicating quasi-reversibility in the redox properties of **L**$^{\bullet}$ and may also be due to a lower electrolyte concentration than for K**L** (0.1 M *vs* 0.14 M). In Cu_2I_2(**L**$^{\bullet}$) the general features of K**L** and **L**$^{\bullet}$ are retained, with two similar reductions seen at +0.07 V and –1.00 V; a new irreversible oxidation at +0.83 V is also seen and is tentatively assigned to Cu^{II}/Cu^{I} oxidation. These data, along with the computed electronic structures, show that the redox reactivity seen in Cu_2I_2(**L**$^{\bullet}$) is primarily ligand-based.

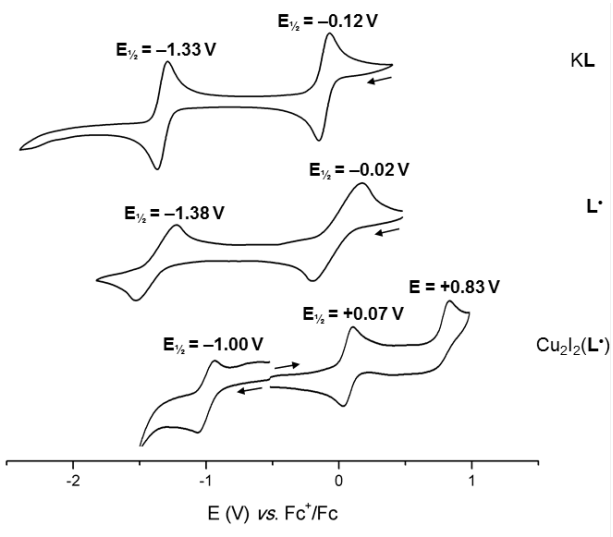

Figure 6. Comparison of CV data for K**L** (top), **L**• (middle), and Cu_2I_2(**L**•) (bottom); glassy carbon working electrode, platinum gauze counter electrode, silver wire *pseudo*-reference electrode, 100 mV s^{-1}, referenced to Fc^+/Fc, 1 mM analyte, 0.1 M – 0.14 M [*n*-Bu_4N][PF_6] electrolyte in dry CH_2Cl_2 under N_2.

We have shown that the thiophene analogue of a N-donor expanded dipyrrin exhibits rich radical chemistry, forming the unusual, isolable neutral radical **L**•, its dicopper complex Cu_2I_2(**L**•), and the radical dication **L**•$^{2+}$. The radical chemistry of thiophenes and their complexes is relatively unexplored and primarily limited to examples in which the radical is stabilized within a macrocyclic framework. As such, this work provides the first insight into new thiophene coordination chemistry which, thanks to the redox activity of this ligand framework, could potentially lead to metal complexes with an internal electron reservoir for redox chemical processes.

Acknowledgements

We thank Dr Carole Morrison for assistance with ELF calculations and the University of Edinburgh and the EPSRC CRITICAT Centre for Doctoral Training (Ph.D. studentship to M.C.; Grant code EP/L016419/1) for financial support. S. S. gratefully acknowledges the Royal Society of Chemistry for a J. W. T. Jones Travelling Fellowship Grant.

Keywords: thiophene • redox-active ligand • density functional theory • dinuclear copper • X-ray crystallography

[1] A. Davison, N. Edelstein, R. H. Holm, A. H. Maki, *Inorg. Chem.* **1963**, *2*, 1227-1232; H. B. Gray, E. Billig, *J. Am. Chem. Soc.* **1963**, *85*, 2019-2020; H. B. Gray, R. Williams, I. Bernal, E. Billig, *J. Am. Chem. Soc.* **1962**, *84*, 3596-3597; G. N. Schrauzer, V. Mayweg, *J. Am. Chem. Soc.* **1962**, *84*, 3221-3221; R. Eisenberg, H. B. Gray, *Inorg. Chem.* **2011**, *50*, 9741-9751; S. Sproules, K. Wieghardt, *Coord. Chem. Rev.* **2010**, *254*, 1358-1382.

[2] C. T. Lyons, T. D. P. Stack, *Coord. Chem. Rev.* **2013**, *257*, 528-540; W. Kaim, B. Schwederski, *Coord. Chem. Rev.* **2010**, *254*, 1580-1588; A. Krężel, W. Maret, *Biochem. J.* **2007**, *402*, 551-558.

[3] J. Jacquet, M. Desage-El Murr, L. Fensterbank, *ChemCatChem* **2016**, *8*, 3310-3316; W. Huang, P. L. Diaconescu, *Inorg. Chem.* **2016**, *55*, 10013-10023; D. L. J. Broere, R. Plessius, J. I. van der Vlugt, *Chem. Soc. Rev.* **2015**, *44*, 6886-6915; M. D. Greenhalgh, A. S. Jones, S. P. Thomas, *ChemCatChem* **2015**, *7*, 190-222; O. R. Luca, R. H. Crabtree, *Chem. Soc. Rev.* **2013**, *42*, 1440-1459; R. F. Munha, R. A. Zarkesh, A. F. Heyduk, *Dalton Trans.* **2013**, *42*, 3751-3766; V. Lyaskovskyy, B. de Bruin, *ACS Catalysis* **2012**, *2*, 270-279; V. K. K. Praneeth, M. R. Ringenberg, T. R. Ward, *Angew. Chem. Int. Ed.* **2012**, *51*, 10228-10234; W. Kaim, *Eur. J. Inorg. Chem.* **2012**, *2012*, 343-348; P. J. Chirik, *Inorg. Chem.* **2011**, *50*, 9737-9740; P. J. Chirik, K. Wieghardt, *Science* **2010**, *327*, 794-795.

[4] V. T. Annibale, D. Song, *RSC Advances* **2013**, *3*, 11432-11449.

[5] J. R. Pankhurst, T. Cadenbach, D. Betz, C. Finn, J. B. Love, *Dalton Trans.* **2015**, *44*, 2066-2070.

[6] J. R. Pankhurst, N. L. Bell, M. Zegke, L. N. Platts, C. A. Lamfsus, L. Maron, L. S. Natrajan, S. Sproules, P. L. Arnold, J. B. Love, *Chem. Sci.* **2017**, *8*, 108-116.

[7] A. Kochem, L. Chiang, B. Baptiste, C. Philouze, N. Leconte, O. Jarjayes, T. Storr, F. Thomas, *Chem. Eur. J.* **2012**, *18*, 14590-14593.

[8] B. K. Reddy, A. Basavarajappa, M. D. Ambhore, V. G. Anand, *Chem. Rev.* **2017**, *117*, 3420-3443; P. Schweyen, K. Brandhorst, R. Wicht, B. Wolfram, M. Bröring, *Angew. Chem. Int. Ed.* **2015**, *54*, 8213-8216; T. Yoshida, W. Zhou, T. Furuyama, D. B. Leznoff, N. Kobayashi, *J. Am. Chem. Soc.* **2015**, *137*, 9258-9261; Y. Tanaka, T. Yoneda, K. Furukawa, T. Koide, H. Mori, T. Tanaka, H. Shinokubo, A. Osuka, *Angew. Chem. Int. Ed.* **2015**, *54*, 10908-10911; C. G. Claessens, D. González-Rodríguez, M. S. Rodríguez-Morgade, A. Medina, T. Torres, *Chem. Rev.* **2014**, *114*, 2192-2277; E. T. Hennessy, T. A. Betley, *Science* **2013**, *340*, 591-595; A. Loudet, K. Burgess, *Chem. Rev.* **2007**, *107*, 4891-4932.

[9] P. Kaszyński, C. P. Constantinides, V. G. Young, *Angew. Chem. Int. Ed.* **2016**, *55*, 11149-11152.

[10] T. Chatterjee, V. S. Shetti, R. Sharma, M. Ravikanth, *Chem. Rev.* **2017**, *117*, 3254-3328.

[11] S. C. Rasmussen, S. J. Evenson, C. B. McCausland, *Chem. Commun.* **2015**, *51*, 4528-4543.

[12] T. Y. Gopalakrishna, J. S. Reddy, V. G. Anand, *Angew. Chem. Int. Ed.* **2014**, *53*, 10984-10987.

[13] A. Wakamiya, T. Nishinaga, K. Komatsu, *Chem. Commun.* **2002**, 1192-1193.

[14] I. Tabakovic, T. Maki, L. L. Miller, Y. Yu, *Chem. Commun.* **1996**, 1911-1912; P. C. d'Oro, A. Mangini, G. F. Pedulli, P. Spagnolo, M. Tiecco, *Tetrahedron Lett.* **1969**, *10*, 4179-4181.

[15] K. Singh, A. Sharma, *Tetrahedron* **2010**, *66*, 3682-3686; T. Kawase, T. Enomoto, C. Wei, M. Oda, *Tetrahedron Lett.* **1993**, *34*, 8143-8146.

[16] T. C. Davenport, T. D. Tilley, *Angew. Chem. Int. Ed.* **2011**, *50*, 12205-12208.

[17] R. Kia, M. Scholz, P. R. Raithby, S. Techert, *Inorg. Chim. Acta* **2014**, *423, Part A*, 348-357; L.-Z. Chen, G.-F. Han, H.-Y. Ye, H.-W. Hu, *Chin. J. Inorg. Chem.* **2010**, *26*, 2541; A. Doshi, K. Venkatasubbaiah, A. L. Rheingold, F. Jakle, *Chem. Commun.* **2008**, 4264-4266; L. Latos-Grazynski, J. Lisowski, M. M. Olmstead, A. L. Balch, *Inorg. Chem.* **1989**, *28*, 1183-1188; C. R. Lucas, S. Liu, M. J. Newlands, J.-P. Charland, E. J. Gabe, *Can. J. Chem.* **1989**, *67*, 639.

[18] A. C. Lane, C. L. Barnes, W. E. Antholine, D. Wang, A. T. Fiedler, J. R. Walensky, *Inorg. Chem.* **2015**, *54*, 8509-8517.